Asteroseismology of the β Cephei star ν Eridani: Interpretation and applications of the oscillation spectrum

A. A. Pamyatnykh[1,2,3],$\star$ G. Handler[3] and W. A. Dziembowski[1,4]

[1] *Copernicus Astronomical Center, Bartycka 18, 00-716 Warsaw, Poland*
[2] *Institute of Astronomy, Russian Academy of Sciences, Pyatnitskaya Str. 48, 109017 Moscow, Russia*
[3] *Institut für Astronomie, Universität Wien, Türkenschanztrasse 17, A-1180 Wien, Austria*
[4] *Warsaw University Observatory, Al. Ujazdowskie 4, 00-478 Warsaw, Poland*

ABSTRACT

The oscillation spectrum of ν Eri is the richest known for any variable of the β Cephei type. We interpret the spectrum in terms of normal mode excitation and construct seismic models of the star. The frequency data combined with data on mean colours sets the upper limit on the extent of overshooting from the convective core. We use data on rotational splitting of two dipole ($\ell = 1$) modes (g_1 and p_1) to infer properties of the internal rotation rate. Adopting a plausible hypothesis of nearly uniform rotation in the envelope and increasing rotation rate in the μ-gradient zone, we find that the mean rotation rate in this zone is about three times faster than in the envelope. In our standard model only the modes in the middle part of the oscillation spectrum are unstable. To account for excitation of a possible high-order g-mode at $\nu = 0.43$ cd^{-1} as well as p-modes at $\nu > 6$ cd^{-1} we have to invoke an overabundance of Fe in the driving zone.

Key words: stars: variables: other – stars: early-type – stars: oscillations – stars: individual: ν Eridani – stars: convection – stars: rotation

1 INTRODUCTION

The rich oscillation spectrum of ν Eri obtained in a recent multisite campaign (Handler et al. 2004, Aerts et al. 2004) holds the best prospects for seismic sounding of the interior of a B-star but also presents a considerable challenge to stellar pulsation theory. The sounding is facilitated by the fact that for several excited modes the spherical harmonic indices were determined (De Ridder et al. 2004). The challenge is to explain mode excitation in an unexpectedly broad frequency range.

The oscillation spectrum of ν Eri is shown in Fig. 1. Before the campaign only the $\ell = 0$ mode and the ($\ell = 1$, g_1) triplet were known. However, for the triplet, the identification of the spherical harmonic was uncertain. Now, thanks to the analysis of accurate multicolour photometry and high-resolution spectroscopy, the uncertainty was eliminated. Reliable information about ℓ is a crucial input for constructing

seismic models of a star, that is, the models constrained by the frequency data.

In this work, we attempt to make the best use of the frequency data to address unsolved problems in stellar evolution theory concerning element mixing in convectively stable layers and angular momentum evolution. The problems are related because rotation induces fluid flows that may cause mixing. It is important to disentangle effects of overshooting from the convective core and effects of rotationally induced element mixing. The first effect depends only on stellar mass. The second one depends on randomly distributed stellar angular momenta. In this context, ν Eridani, which is a very slowly rotating B star, yields a useful extreme case. However, it would be important to try to obtain similar quality data for more rapidly rotating objects.

We are very curious how the angular velocity of rotation behaves in stellar interiors. Let us remind that, while the results of helioseismic sounding of radial structure essentially confirmed the standard solar model, the results for the internal rotation rate came as a surprise. The outstanding
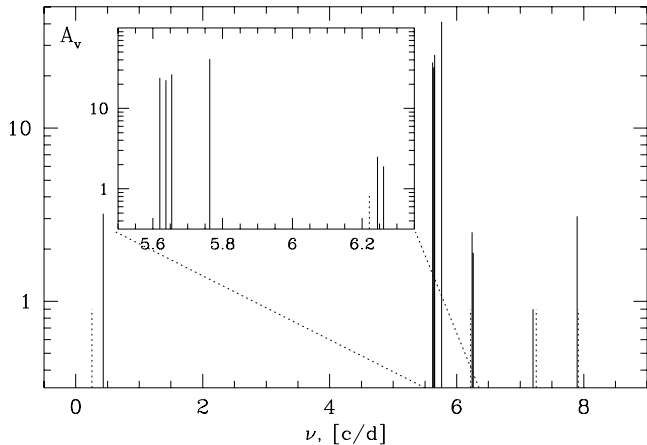
$\star$ E-mail: alosza@camk.edu.pl

Figure 1. Oscillation spectrum of ν Eri. The peaks represented with the broken vertical lines are regarded uncertain. The four modes known before the campaign are between $\nu = 5.6$ and 5.8 cd^{-1}. De Ridder et al. (2004) identified them as an $\ell = 1$ triplet and an $\ell = 0$ singlet. The newly discovered triplet at $\nu \approx 6.25$ cd^{-1} is identified as $\ell = 1$ (De Ridder et al. 2004). In this paper we will show that the radial mode is the fundamental and the two dipole modes are g_1 and p_1, respectively. Only these mode frequencies are used in our seismic sounding.

question in the case of massive stars is whether a substantial radial gradient of the angular rotation rate may be present in their interiors. The question is related to another very interesting and important problem which is the origin of magnetic fields in B type stars.

A seismic model of a pulsating star should not only account for the measured frequencies but also for the instability of the detected modes. The latter requirement sets a different kind of constraint than the former as it concerns only properties of the outer layers, where most of contribution to mode driving and damping arises. Since the frequency spectrum of ν Eri seems unusually broad for an object of its type, constraints in this case are particularly interesting.

The structure of this paper is as follows. In Sect. 2 we construct models of the internal structure for ν Eri and calculate its oscillation frequencies. We find models for which the oscillation frequencies of three $m = 0$ modes – $(\ell = 0, p_1)$, $(\ell = 1, g_1)$ and $(\ell = 1, p_1)$ – reproduce the observations as well as have effective temperatures and luminosities within the observational error box. In Sect. 3 we use these models and data on the triplet structure to infer the internal rotation of the star.

The problem of how to make the observed modes pulsationally unstable is discussed in Sect. 4. The tasks of constructing the model of ν Eri whose mode frequencies match the data and of the identification of the driving effect are not quite independent. The driving effect in B stars strongly depends on the iron content and its distribution in outer layers. In Sect. 5, we study how modification of the iron distribution affects the frequencies. We also propose plausible identifications of all modes detected in the ν Eri oscillation spectrum.

2   MODEL OF THE STELLAR INTERIOR

For the purpose of constructing models of ν Eri we ignored all effects of rotation which, as we have checked, was fully

justified. Accordingly, we make use here only of the $m = 0$ mode frequencies despite, in general, rotation causes a shift of the centroid frequency. We consider models of massive main sequence stars in the phase of radius expansion. A model is characterised by its mass, M, effective temperature, $T_{\rm eff}$, initial hydrogen, X, and heavy element, Z, abundance, as well as the overshooting parameter, $\alpha_{\rm ov}$. Here we assume the standard solar mixture of heavy elements (departures will be considered in section 5) and fix X at 0.7. For opacity and the equation of state we use the OPAL tabular data (Iglesias & Rogers 1996, Rogers et al. 1996). The nuclear reaction rates are the same as used by Bahcall and Pinsonneault (1995).

2.1 ν Eridani's position in the theoretical H-R diagram

The position of the star in the $\log T_{\rm eff} - \log L$ diagram is not very accurately known. Our temperature determination is based on Strömgren photometry and on the tabular data by Kurucz (1998). For L we use the Hipparcos parallax, Lutz-Kelker correction to the absolute magnitude (Lutz & Kelker 1973), and the bolometric correction from Kurucz's data. In this way we obtained the following numbers

$$\log T_{\rm eff} = 4.346 \pm 0.011 \quad \text{and} \quad \log L = 3.94 \pm 0.15.$$

For $\log T_{\rm eff}$ we include measurement errors and uncertainty of calibration. For $\log L$ we take into account errors of the parallax and uncertainty of the bolometric correction. Our numbers are similar to those quoted by Dziembowski & Jerzykiewicz (2003) and will be updated by De Ridder et al. (2004).

2.2   Identification of the radial overtone of the observed modes

Before starting seismic modelling of ν Eri, we must complete the mode identification. The work by De Ridder et al. (2004) provided unambiguous ℓ identifications for seven modes, and m determinations by inference, but the radial overtone of the modes has not been determined. Fortunately, one of the detected pulsation modes is radial, which eases this task considerably.

Consequently, we follow Dziembowski & Jerzykiewicz (1996) and only consider two one-dimensional families of models. The position of ν Eri in the HR diagram is only consistent with the radial mode at 5.7634 cd^{-1} being the fundamental or the first overtone (as indicated later in Fig. 3). For these two possibilities, we examine the mass dependence of theoretical $\ell = 1$ mode frequencies of standard models and match it to the observed $\ell = 1$ mode frequencies (Fig. 2).

Because of the mixed-type character of some of the modes we can only match the observed frequencies of the two lowest-order $\ell = 1$ modes within certain mass ranges. However, under the assumption of the radial mode being the first overtone, no acceptable fit can be found for the $\ell = 1$ mode of highest frequency. Hence we can eliminate this possible identification (which would also be less consistent with the star's position in the HR diagram) and identify the radial pulsation mode of ν Eri as the fundamental. Consequently, the $\ell = 1$ modes are the first g-mode (g_1) and the first two

Table 1. Parameters of fitted models. The symbols denote : X_c – hydrogen abundance in the core, M_{mix} – mass of the mixed core, which is the same as mass of the convective core at $\alpha_{ov} = 0$, r_c – radius of the convective core, r_{c0} – radius of the convective core at ZAMS, which corresponds to the top of the μ-gradient zone.

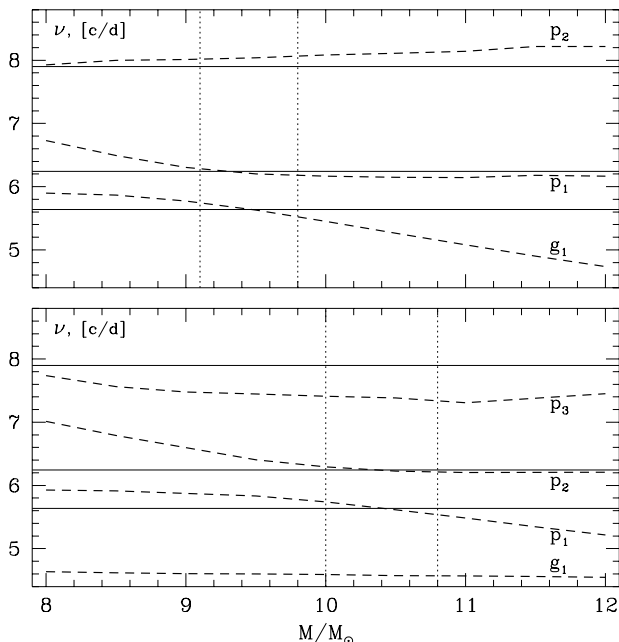| $M/M_\odot$	α_{ov}	Z	age[My]	$\log T_{eff}$	$\log L$	$R/R_\odot$	$\log g$	X_c	M_{mix}/M	r_c/R	r_{c0}/R
9.858	0.0	0.015	15.7	4.3553	3.969	6.279	3.836	0.2414	0.189	0.117	0.186
9.179	0.1	0.015	18.9	4.3399	3.891	6.165	3.821	0.2555	0.211	0.121	0.185

Figure 2. Identification of the radial overtone of the observed modes of ν Eri. We assume the radial mode to be the fundamental in the upper panel and to be the first overtone in the lower panel. The mass dependence of theoretical $\ell = 1$ mode frequencies (dashed lines) is compared to the observed $\ell = 1$ mode frequencies (horizontal lines). We find two ranges in mass (denoted by the vertical dotted lines) where the two $\ell = 1$ modes of lowest frequency match the observed frequencies well. However, the $\ell = 1$ mode near 7.9 cd^{-1} can only be reproduced in the case of the radial mode being the fundamental.

p-modes (p$_1$ and p$_2$). We note that the theoretical fit of the standard model to the observed p$_2$ mode is also not very satisfactory at first glance; we will return to this problem and its possible solution later.

2.3 Fitting frequencies of the $\ell = 0$ and two $\ell = 1, m = 0$ modes

We calculated frequencies of these three modes in evolutionary sequences of stellar models characterised by the parameters M, Z, α_{ov}. The first two of them and T_{eff} were regarded as adjustable parameters to fit the measured frequencies. The adopted precision of the fit was 10^{-3}. The precision of the data is much higher but matching to such a precision is neither interesting nor reasonable in view of the uncertainties of the model calculations, such as the limited accuracy of the opacity data. The upper limit of the
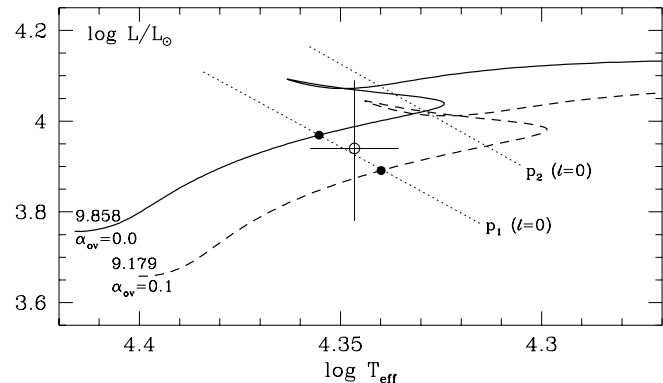

Figure 3. The evolutionary tracks for the models fitting frequencies of the $(\ell = 0, p_1)$, $(\ell = 1, g_1)$ and $(\ell = 1, p_1)$ modes in ν Eri. Models were calculated with chemical composition parameters $Z = 0.015$ (adjusted) and $X = 0.7$ (fixed). The values of M and α_{ov} are indicated. The values of T_{eff} and $\log L$ inferred from photometry and the Hipparcos parallax are shown with the error bars. Two dotted lines connect models with 5.7633 c/d as the radial fundamental (p$_1$) and first overtone (p$_2$) mode.

α_{ov} parameter was derived from the bounds on the effective temperature.

We obtained models with $\alpha_{ov} = 0.0$ and $\alpha_{ov} = 0.1$ which satisfy all the observational constraints. The inferred value of the metallicity parameter is $Z = 0.0150 \pm 0.0001$, the same at $\alpha_{ov} = 0.0$ and 0.1. Parameters of the two selected models are given in Table 1.

Both models are well within the error box in the theoretical H-R diagram shown in Fig. 3. Increasing α_{ov} above 0.12 would place the seismic model below the lower bound of T_{eff}. We, thus, conclude that the data on ν Eri are consistent with negligible overshooting distance and set an upper bound on it at $\alpha_{ov} = 0.12$. Further constraining the extent of overshooting may be possible when the effective temperature determination is improved. Our constraint is in agreement with $\alpha_{ov} = 0.10 \pm 0.05$ derived by Aerts et al. (2003) from frequency analysis for the β Cephei star HD 129929, which is also slowly rotating.

The frequency distance between the $(\ell = 1, g_1)$ and $(\ell = 0, p_1)$ modes is indeed a very sensitive probe of overshooting. This is illustrated in Fig. 4, where we show the evolution of the three mode frequencies as a function of T_{eff}. This is the main application of the $(\ell = 1, g_1)$ mode. However, without the $(\ell = 1, p_1)$ mode frequency the assessment of α_{ov} would not be possible unless we have an accurate observationally determined Z value which we do not.
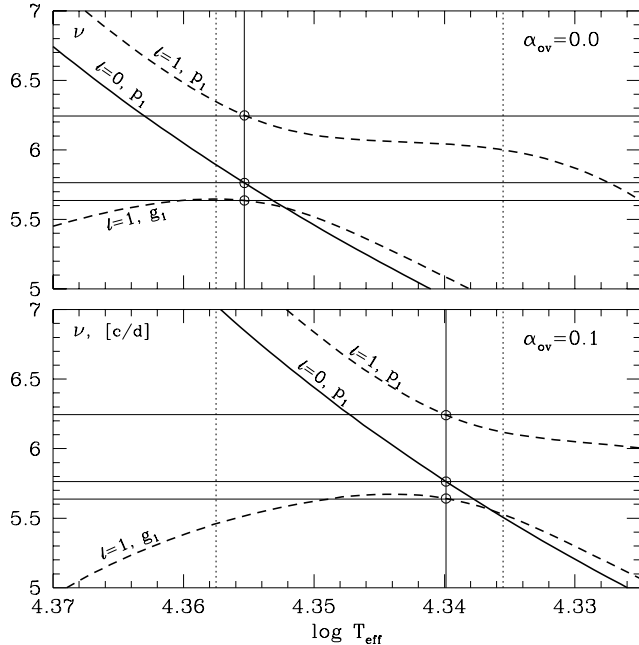
Figure 4. The evolution of the calculated frequencies of the selected modes in the model sequences shown in Fig. 2. Two dotted vertical lines mark the allowed T_{eff} range. Three horizontal lines correspond to the measured frequencies. Solid vertical lines correspond to T_{eff} for the fitted models. The fittings are marked by open circles. Note that the g_1 mode frequency comes close to the radial mode frequency in a very narrow range of T_{eff} and the location of this range is very sensitive to α_{ov}. Crossing of the two frequencies takes place at the point of the minimum frequency distance between the two $\ell = 1$ modes (avoided crossing). Before the avoided crossing, the $(\ell = 1, \mathrm{p}_1)$ mode is nearly a pure acoustic mode with its frequency evolution line being nearly parallel to the corresponding line for the radial mode. The ratio of the two frequencies depends on Z.

2.4 Probing properties of low order $\ell = 1$ modes

It is remarkable how much the three mode frequencies tell us about the star's internal structure. Identification of a radial mode is important because its frequency yields an accurate constraint on the model parameters; however, much more interesting is the information contained in the $\ell = 1$ modes.

The probing property of a mode depends on the distribution of its oscillation energy, E, in the stellar interior. The plots in the upper panel of Fig. 5 show $\mathcal{E}$, the energy derivative with respect to the fractional radius, for the four consecutive $\ell = 1$ modes. In spite of rather close frequencies, modes g_1 and p_1 have a grossly different distribution of energy. This explains the differences in their evolution seen in Fig. 4 as well as the difference in the probing properties. One should also notice the peculiar $\mathcal{E}(r)$ dependence for the g_1 and p_1 modes in the deep interior. A maximum (absolute in the former and local in the latter case) is reached at the boundary of the convective core where the Brunt-Väisälä frequency has a derivative discontinuity. The g_2 and all higher order g-modes have the maxima within the propagation zone. For our models it is the g_1 mode whose frequency is most sensitive to overshooting. In more evolved models this property will shift to p_1. Dziembowski & Pamyatnykh (1991) observed this property of certain low order
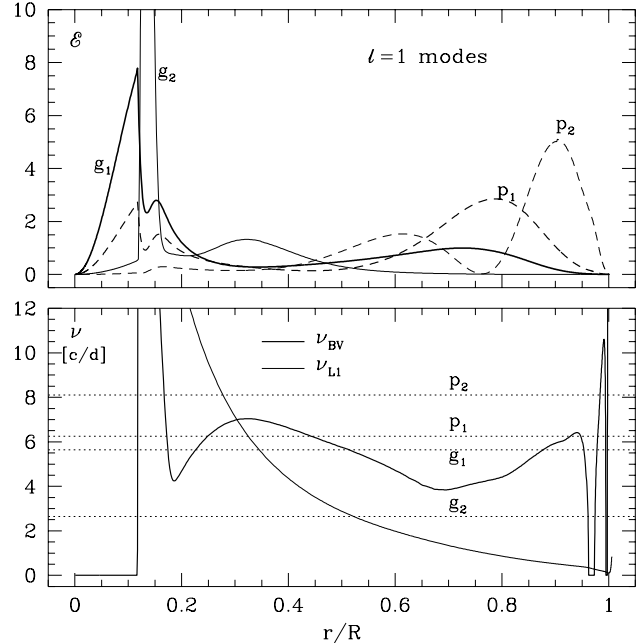

Figure 5. *Upper panel:* Oscillation energy distribution, $\mathcal{E}$, for low order $\ell = 1$ modes in the ν Eri model calculated with $\alpha_{\mathrm{ov}} = 0$. The plots are very similar in the models with $\alpha_{\mathrm{ov}} = 0.1$. *Lower panel:* The Brunt-Väisälä frequency, ν_{BV}, and the Lamb frequency at $\ell = 1$, ν_{L1}, in the same model.

g-modes, called by them g_c, in δ Scuti star models, and emphasized the importance of detecting such a mode in the context of the overshooting problem. ν Eri is the first object in which a g_c mode was definitely detected. More than that, its rotational splitting has been measured.

ν Eridani is not exceptional amongst β Cep stars, which are $9 - 12 M_{\odot}$ stars in the advanced main sequence phase of evolution. In models of such stars we typically find that the $(\ell = 1, g_1)$ and $(\ell = 1, p_1)$ modes are both unstable. There are chances that they will be detected in a number of other stars of this type. The good luck in the case of ν Eri is that we capture it before the avoided crossing of the $\ell = 1$ modes. After it, the data on the modes yield much less orthogonal information.

3 INTERNAL ROTATION

3.1 The $\ell = 1$ triplets

The frequency structure of a rotationally split $\ell = 1$ mode may be characterised by the mean splitting $S = 0.5(\nu_{+1} - \nu_{-1})$ and the asymmetry $A = \nu_{-1} + \nu_{+1} - 2\nu_0$. If all effects of higher order in the angular rotation rate, Ω, as well as effects of a magnetic field are negligible, then $A = 0$. Both parameters, A and S, for the g_1 mode have been determined before the present campaign (Dziembowski & Jerzykiewicz 2003).

If we allow only an r-dependence in Ω then

$$\nu_m = \nu_0 + \frac{m}{2\pi} \int_0^R \frac{dr}{R} \mathcal{K}\Omega + D_0 + m^2 D_1.$$

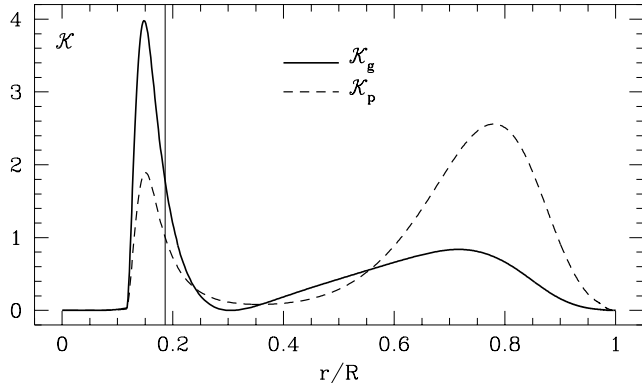The rotational splitting kernel, $\mathcal{K}$, is given by

Figure 6. The rotational splitting kernel for the g_1 and p_1 modes in the model calculated with $\alpha_{\rm ov} = 0$. The vertical line at r_{c0}/R marks the top of the μ-gradient zone. Note the difference between $\mathcal{K}$ and $\mathcal{E}$, shown in Fig. 5. Rotation within the convective core has hardly any effect on the $\ell = 1$ splitting.

$$\mathcal{K} = \frac{(\xi_r^2 - 2\xi_r\xi_h + [\ell(\ell+1) - 1]\xi_h^2)r^2\rho}{\displaystyle\int_0^R \frac{dr}{R}[\xi_r^2 + \ell(\ell+1)\xi_h^2]r^2\rho}, \qquad (1)$$

where ξ_r and ξ_h are defined by the following expression for the displacement eigenvector

$$\vec{\xi} = (\xi_r\vec{e}_r + \xi_h\vec{\nabla}_h)Y_\ell^m.$$

The kernels for the two modes considered are shown in Fig. 6. The quantities D_0 and D_1 are quadratic in Ω. The asymmetry of the triplet arising from the quadratic effect of rotation is $2D_1$. The quantity D_0 represents the frequency shift of the $m = 0$ mode. As we have mentioned in section 2.1, in principle, this shift should be subtracted from the measured frequencies of $m = 0$ modes when we fit frequencies calculated for a spherical model.

From the frequencies listed by Handler et al. (2004) for the g_1 mode we derive $S_g = 1.69 \times 10^{-2}$ cd^{-1} (from here on we use subscript g to denote quantities referring to the g_1 mode, those referring to the p_1 mode will be subscribed with p), which is nearly the same as before (Dziembowski & Jerzykiewicz 2003). There is, however, a significant difference in the asymmetry for which the previous value was $A_g = -7.1 \times 10^{-4}$ cd^{-1}, but from the most recent data we now determine a value which is by more than a factor of two smaller. The former value was larger than calculated assuming uniform rotation with the rate inferred from S_g. Dziembowski & Jerzykiewicz (2003) considered two possible solutions. One was faster rotation in the envelope than in the interior, the second was a contribution to D_1 from a hypothetical magnetic field. The current data taken in a 158 day-long campaign and their time distribution are insufficient for a precise determination of A_g. Thus we will not use this parameter here and we will not consider effects of a possible magnetic field. We will postpone interpretation of the A_g value until we have more precise determination from the future data analysis.

For the p_1 mode we have reliable frequencies only for the $m = 0$ and $+1$ components. The frequency of the $m = -1$

component may be estimated from the value of A_g, assuming that D_1 arises from the second order effect of rotation with the same rate for both modes. In this way we get (assuming A_g from earlier data which we regard as more reliable)

$$A_p = A_g \frac{D_{1,p}}{D_{1,g}} = -1.13 \times 10^{-3} \text{ cd}^{-1}$$

and

$$\nu_{-1,p} = 2\nu_{0,p} - \nu_{+1,p} + A_p = 6.2250 \text{ cd}^{-1}.$$

We stress that choosing A_g from newer data or setting $A_g = 0$ will make very small difference. In a similar manner we find a frequency shift $D_{0,p} = 7 \times 10^{-4}$ for the $m = 0$ mode. The number is below the adopted precision of the frequency fit in our model construction. For the linear rotational frequency splitting we get

$$S_p = \nu_{+1,p} - \nu_{0,p} - 0.5A_p = 0.01797 + 0.00056 = 0.0185\text{cd}^{-1}$$

3.2 Rotation rate in the envelope and in the μ-gradient zone

Since we have data on rotational splitting only for two modes, our inference on the internal rotation must rely on simplifying assumptions. Results from seismic sounding of the solar internal rotation suggest that within chemically homogeneous radiative layers the rotation rate should be close to uniform. A possible steep gradient may occur only in the chemically inhomogeneous zone around the convective core, where the μ-gradient stabilises differential rotation. With this in mind, we write

$$2\pi S_g = K_{c,g}\bar{\Omega}_c + K_{e,g}\bar{\Omega}_e$$

and

$$2\pi S_p = K_{c,p}\bar{\Omega}_c + K_{e,p}\bar{\Omega}_e,$$

where

$$K_{c,j} = \int_0^{r_{c0}} \frac{dr}{R}\mathcal{K}_j, \qquad K_{e,j} = \int_{r_{c0}}^R \frac{dr}{R}\mathcal{K}_j,$$

and $j \equiv p$ or g. In our fitted models we have

$$K_{c,g} = 0.187(0.168), \qquad K_{e,g} = 0.345(0.395)$$

$$K_{c,p} = 0.092(0.101), \qquad K_{e,p} = 0.718(0.682),$$

where numbers in brackets refer to the model calculated with $\alpha_{\rm ov} = 0.1$. The results are nearly the same for both models. We find

$$\bar{\Omega}_c \approx 3\bar{\Omega}_e.$$

Figure 6 shows the averaging kernels for Ω. The fact that the convective core virtually does not contribute to the splitting is an exclusive property of $\ell = 1$ modes which may be easily seen by considering the behaviour of eigenfunctions near the $r \to 0$ singularity. For finite $\vec{\xi}$'s we have then $\xi_r \to \ell\xi_h$, implying (see Eq.(1)) $\mathcal{K} \to 0$ if $\ell = 1$. Thus, the value $\bar{\Omega}_c$ refers only to the μ gradient zone. It is clear that our result implies a very sharp decline of the rotation in the layer between the current core boundary and that at the ZAMS phase. How sharp the decline is depends on the form of the $\Omega(r)$ dependence. A factor ~ 5 is derived if we assume

a linear decrease of Ω between $r = r_c$ and r_{c0} and constant Ω for $r > r_{c0}$.

With this simple form of $\Omega(r)$ we find an equatorial velocity of rotation $v_e = 6.1$ km/s, which is 2/3 of the value inferred from S_g on the assumption of uniform rotation. Since the quadratic effect of rotation is still expected to arise mainly above $r = r_c$, we have a problem with accounting for the pre-campaign value of A_g. The values of the asymmetries calculated ignoring the contribution from below $r = r_{c0}$ are $A_g = -2.0 \times 10^{-4}$ and $A_p = -2.6 \times 10^{-4}$. The time for a new discussion of the triplet asymmetry will come when we have more precise frequencies of the modes in both triplets.

4   HOW THE MODES EXCITED IN ν ERI ARE DRIVEN

Oscillation driving in B-type stars seems rather well understood (see e.g. Pamyatnykh 1999). For low ℓ modes theory predicts the occurrence of two instability domains within the main sequence band. In models of stars with earlier spectral types (B1 - B3) low order p- and g-modes are pulsationally unstable, as found in β Cep stars, and in stars with later spectral types (B4 - B8) high order g-modes are predicted unstable, typically found in SPB stars. ν Eri is perhaps the first β Cep star where both kinds of modes are present (Handler et al. 2004). In the following, we assume that the 0.432 cd^{-1} signal in the light curves of ν Eri is an independent pulsation mode. There is a slight chance that it may be a combination signal, but its required order would be much higher than those of all the observed combination frequencies of similar amplitude. Thus we regard such an interpretation highly unlikely.

In our fitted models we find unstable modes only in the $4.0 - 6.5$ cd^{-1} frequency range. The instability measure, η, plotted in Fig. 7, is not a monotonic function of frequency. There is a noticeable maximum of the instability measure near $\nu = 0.5$ cd^{-1} for the $\ell = 1$ sequence and at somewhat higher frequency for $\ell = 2$. The existence of this maximum suggests that pulsational instability in this part of the eigenmode spectrum may be found upon some modification of our models.

Our proposal for extending the instability range is not original. We follow the idea of Charpinet et al. (1996, 1997) and Fontaine et al. (2003) that the combined effect of settling and radiative levitation may lead to significant overabundance of iron in the driving zone. Since we do not have a stellar evolution code treating these effects, we simply introduced an *ad hoc* factor 4 enhancement of the iron-group elements in the $\log T$ range $5.1-5.5$ and matched it smoothly to the standard solar value outside. The result is shown in Fig. 7. We may see that, while an extension of the instability to higher order p-modes is easy, obtaining instability in the high-order g-mode range is more difficult. We found unstable $\ell = 2$ g-modes in the model calculated with $\alpha_{ov} = 0.1$, which is cooler, but only at $\nu \approx 0.8$ cd^{-1}. Because of the *ad hoc* nature of the proposed iron enhancement we regard these results merely as an indication of a direction where the solution of the driving problem of modes detected in ν Eri may be found. The proposal that the diffusion effects may play a role in this star seems not unreasonable in view of its
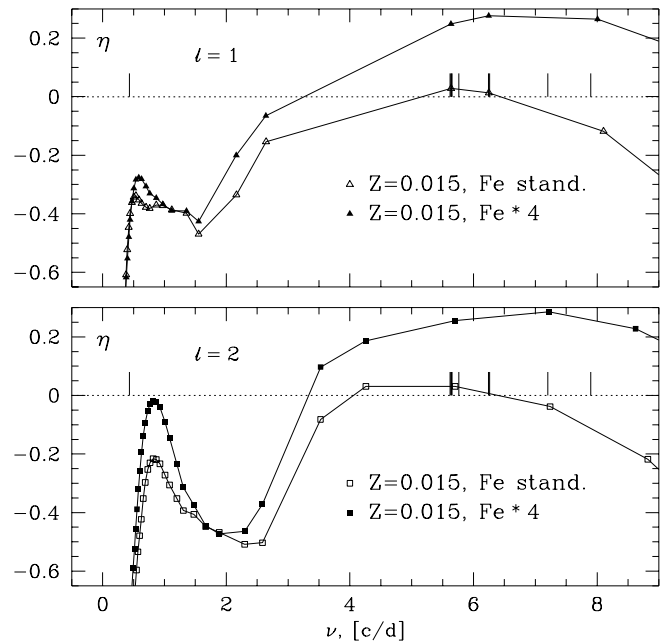

Figure 7. The instability measure, η, for $\ell = 1$ and $\ell = 2$ modes in a standard model calculated with $\alpha_{ov} = 0$ and in the corresponding model with the Fe enhancement in the driving zone. $\eta > 0$ for unstable modes. $\eta = -1$ if there is no active driving layer in the star for a particular mode and it is $+1$ if driving occurs in the whole interior. The position of the modes detected in ν Eri are marked with bars on the $\eta = 0$ axis.

very slow rotation which should not induce any appreciable mixing of elements and this is the first star where modes in such a broad frequency range were detected. However, slow rotation cannot be the sufficient condition for a broad-band excitation. In HD 129929, which is even a slower rotator, all modes detected so far are confined to the narrow frequency range of 6.45 - 7 cd^{-1} .

5   POSSIBLE IDENTIFICATION OF THE REMAINING MODES

Our manipulations on the Fe abundance in outer layers are not without consequences for mode frequencies and hence on the seismic model of ν Eri. It is not difficult to find a model with modified Fe which fits the three frequencies used in section 2.1. The model cannot be very different; however, the frequencies of higher order p-modes are more significantly changed.

Let us begin with the possible mode at $\nu = 0.432$ cd^{-1}. Though it is easier to find instability at higher degrees, the $\ell = 1$ identification seems more plausible because in this case the maximum of η occurs closer to the observed frequency. Assuming $\ell = 1$ and the rotational splitting the same as in the ($\ell = 1$, g$_1$) mode, we obtained 0.429 and 0.435 cd^{-1} for the frequency of the ($\ell = 1, m = -1$, g$_{16}$) mode in the models with $\alpha_{ov} = 0$ and 0.1, respectively. Thus, we regard such an identification for the $\nu = 0.432$ cd^{-1} peak as likely.

For the observed variation at $\nu = 7.20$ cd^{-1}, the only possible identification, regardless of the choice of α_{ov} and modification in the Fe abundance, is a mode of the

$(\ell = 2, p_0)$ quintuplet. In this case the effect of the Fe enhancement is more significant. The enhancement described in the previous section leads to a frequency decrease by 0.02, which is comparable with the rotational splitting. With this model the best fit is for $m = 1$, while with the standard models it is for $m = 2$.

The effect of the Fe enhancement increases with mode frequency. This is not surprising because the acoustic propagation zone expands to outer layers where the effect of the enhancement is largest. For the observed mode at $\nu = 7.90$ cd^{-1} we know the ℓ-value from photometry, and it is 1. In our standard seismic models the $\ell = 1, p_2$ modes have frequencies 8.10 and 8.03 cd^{-1} in models with $\alpha_{\rm ov} = 0$ and 0.1, respectively. In this case, even with the freedom in choosing the m value we cannot reproduce the measured frequency. The frequency shift due to the Fe enhancement, which is about 0.1 cd^{-1}, brings the calculated frequencies close to the fit. We regard this fact as partial support for the proposed effect.

We note that fitting the frequencies of all the modes detected in the 5.6 - 7.9 cd^{-1} frequency range is possible in standard evolutionary models if one allows lower effective temperature and overshooting in the range $0.2 < \alpha_{\rm ov} < 0.3$ (Ausseloos et al. 2004).

6   CONCLUSIONS AND DISCUSSION

We believe that our seismic models of ν Eridani yield a good approximation to its internal structure and rotation but there is room for improvement and a need for a full explanation of mode driving. We did not fully succeed in the interpretation of the oscillation spectrum of ν Eridani with our standard evolutionary models and our linear nonadiabatic treatment of stellar oscillations. We fail to reproduce mode excitation in the broad frequency range, as observed, and to reproduce the frequency of the $(\ell = 1, p_2)$ mode, associated with the highest frequency peak in the spectrum. We showed that both problems may be cured by allowing an enhancement of the iron abundance in the zone of the iron-opacity bump. The enhancement may result from effects of radiative levitation, as first proposed by Charpinet et al. (1996, 1997) to explain oscillations in sdB stars. Our proposal is based on models with an *ad hoc* iron enhancement in the bump zone and must be checked with use of stellar evolution codes that take into account effects of levitation and diffusion of chemical elements. We regard this as the most timely theoretical work aimed at the interpretation of ν Eridani.

The proposed modification concerns only the outer layers and has a small effect on models of the stellar interior and the frequencies of g and p_1 modes. Therefore we believe that our seismic models describe the deep internal structure of the star. These models reproduce frequencies of the fundamental radial modes and two $\ell = 1$ modes and have effective temperatures and luminosities within the measurement error box. Satisfactory models exist in a range of the overshooting parameter, $\alpha_{\rm ov} = (0 - 0.12)$, which corresponds to the mass range $(9.9 - 9.0)M_\odot$, age range $(16 - 20)$ My, and a fractional hydrogen depletion in the core range $(0.34 - 0.38)$. Here the important finding is the upper limit for the extent of overshooting. There is a prospect for getting a more stringent constraint on $\alpha_{\rm ov}$ with a more accurate determination of the star's effective temperature.

We believe that our most important finding concerns internal rotation. We presented evidence for a sharp decline of the rotation rate, Ω, through the μ-gradient zone, around the shrinking convective zone. With data on the splitting for only two $\ell = 1$ modes, our estimates had to rest on the assumed form of the $\Omega(r)$ dependence. Since a significant gradient of Ω is possible only in the μ-gradient zone, we adopted a constant Ω above it (rotation within the convective core has a negligible influence on the splitting). With this simplification we found that data require a decline by a factor ~ 5 within the zone and an equatorial velocity of about 6 km/s. The second order effect from this slow rotation in the envelope cannot account for the asymmetry of the $(\ell = 1, g_1)$ triplet as determined from the pre-campaign data. Only with new observations we will be able to tell whether the problem is real. Our star is not the first β Cephei star for which evidence for nonuniform rotation was put forward. However, we believe that in the ν Eri case the evidence is significantly stronger than in the case of HD 129929 (Aerts et al., 2003), because we relied on splitting data for modes having very different probing kernels.

ν Eridani proved to be a very important pulsating star. After the Sun, it so far is perhaps the most rewarding main sequence object for asteroseismology. Many more modes were detected in several δ Scuti stars but in none of them so many modes have unambiguously been identified. This star deserves continued observational efforts. An extended data base is needed for precise determination of the frequencies of the modes in the $\ell = 1$ triplets. This is important for a more credible assessment of differential rotation. In this context it would be important to obtain a precise value of the projected equatorial velocity of rotation from spectroscopy. The best $v \sin i$ value currently available (Aerts et al. 2004) is higher than that of equatorial velocity inferred in this work which may however be in part due to the combined effects of pulsational and thermal line broadening.

This paper has been typeset from a TeX/ LaTeX file prepared by the author.

REFERENCES

Aerts C., Thoul A., Daszynska J., Scuflaire R., Waelkens C., Dupret M. A., Niemczura E., Noels A., 2003, Science, 300, 1926
Aerts C. et al., 2004, MNRAS, 347, 463
Ausseloos M., et al., 2004, MNRAS, in preparation
Bahcall J. N., Pinsonneault M. H. 1995, Rev. Mod. Phys, 67, 781
Charpinet S. et al., 1996, ApJ, 471, L103
Charpinet S. et al., 1997, ApJ, 483, L123
De Ridder J., Telting J. H., Balona L. A., Handler G., Briquet

M., Daszynska J., Lefever K., Aerts C., 2004, MNRAS, in preparation

Dziembowski W. A., Jerzykiewicz M., 2003, in *Magnetic Fields in O, B and A stars: Origin and Connection to Pulsation, Rotation and Mass Loss*, ASP Conf. Ser., Vol. 305, in press

Dziembowski W. A., Jerzykiewicz M., 1996, A&A, 306, 436

Dziembowski W. A., Pamyatnykh A. A, 1991, A&A, 248, L11

Fontaine G. et al., 2003, ApJ, 597, 518

Handler G., et al., 2004, MNRAS, 347, 454

Iglesias C. A., Rogers F. J. 1996, ApJ, 464, 943

Kurucz R. L., 1998, http://kurucz.harvard.edu/grids.html

Lutz T. E., Kelker D. H. 1973, PASP, 85, 573

Pamyatnykh A. A, 1999, Acta Astr., 49, 119

Rogers F. J., Swenson F. J., Iglesias C. A. 1996, ApJ, 456, 902